ELSEVIER

Ceramics International 32 (2006) 451–455

CERAMICS INTERNATIONAL

www.elsevier.com/locate/ceramint

Water vapor corrosion behavior of lutetium silicates at high temperature

Shunkichi Ueno *, D. Doni Jayaseelan, Tatsuki Ohji

Advanced Manufacturing Research institute, National Institute of Advanced Industrial Science and Technology, 2266-98 Shimo-Shidami, Moriyama-ku, Nagoya 463-8687, Japan

Received 25 September 2004; received in revised form 14 February 2005; accepted 12 March 2005
Available online 30 June 2005

Abstract

The corrosion behavior of hot-pressed lutetium disilicate ($Lu_2Si_2O_7$) bulk sample in static state water vapor environment was examined at 1300 °C. The apparent corrosion rate was estimated as 1.427×10^{-6} g/cm^2 h. The X-ray diffraction pattern showed a trace of Lu_2O_3 phase on the sample surface after corrosion test. SEM observation on the surface of the sample after corrosion test revealed that the surface morphology was not homogeneous but showing three different types of features. During high-temperature water vapor corrosion, lutetia-rich component first melted, and then removed from the grain surface by water vapor attack. Later, the excess boundary silica phase was removed by water vapor corrosion. These underlying corrosion mechanisms of bulk lutetium disilicate sample in static state water vapor environment were discussed in detail.

Keywords: B. Surface; C. Corrosion; D. Silicate; E. Thermal applications

1. Introduction

Silicon nitride ceramics that have high strength at high temperatures have become recently candidate materials for industrial high temperature application, especially, for gas turbine components power plant industry [1,2]. Nevertheless, silicon nitride ceramics oxidize above 800 °C and silica phase is formed on the surface. As silica phase is easily corroded by water vapor at high temperatures [3,4], oxidation resistant coating in the form of environmental barrier coating (EBC) system is necessary for the application of silicon nitride ceramics as gas turbine components.

In consideration of EBC materials, the coefficient of thermal expansion (CTE) of EBC materials must be near to that of silicon nitride ceramics, which is about 4×10^{-6}/°C. This is one of the short selections for choosing a candidate EBC system. As the CTE of rare earth di-silicates ($Ln_2Si_2O_7$, Ln = rare earth elements) are very near to that of silicon nitride ceramics [5], $Lu_2Si_2O_7$ system was chosen as better choice to be used as EBC layer for silicon nitride ceramics. The other reason for choosing especially $Lu_2Si_2O_7$ is, in recent preparation methods, Lu_2O_3 and SiO_2 are being used as sinter additives for silicon nitride ceramics that eventually form $Lu_2Si_2O_7$ phase as the grain boundary phase during sintering at high temperature.

Along these lines, our main interests recently focused on developing high dense EBC layer for silicon nitride ceramics, especially $Lu_2Si_2O_7$ EBC layer. Previously, we reported the water vapor corrosion behavior of silicon nitride ceramics with high dense Lu–Si–O EBC layer [6]. The silicon nitride substrate was well protected by the Lu–Si–O EBC layer at high temperature [6]. However, the corrosion mechanisms of this phase were not clearly studied.

Commonly, silicate compounds have silica or silica-rich phase at the grain boundary. Monteverde and Gelotti reported that 13 mol% excess silica is needed for the preparation of single phase $Ln_2Si_2O_7$ (Ln = rare earth) [7]. Their experimental results indicated that excess silica occurs at the grain boundary of rare earth di-silicates. Hence, this

* Corresponding author. Tel.: +81 527390135; fax: +81 527390136.
E-mail address: shunkichi.ueno@aist.go.jp (S. Ueno).

0272-8842/$30.00
doi:10.1016/j.ceramint.2005.03.022

paper reports water vapor corrosion for hot-pressed $Lu_2Si_2O_7$ at 1300 °C and the corrosion mechanisms of $Lu_2Si_2O_7$ crystal grain and the boundary silica phase are discussed.

2. Experimental

High purity Lu_2O_3 (99.99% purity, Shin-Etsu Chemical Co. Ltd., 4 μm particle size) and SiO_2 (99.99% purity, High Purity Chemicals Co. Ltd., 0.8 μm particle size) powders were used as the starting materials. A stoichiometric molar ratio of these powders Lu_2O_3:SiO_2 = 1:2 were mixed in an agate mortar. The mixed powders were hot pressed at 1600 °C for 3 h in Ar atmosphere at a pressure of 20 MPa. The sintered bulk was cut into rectangular bars of dimension 40 mm × 4 mm × 3 mm.

The high temperature water vapor corrosion test was performed using a Corrosion Testing Machine (Japan Ultra-high Temperature Materials Research Center). The sample was placed on a high purity Al_2O_3 plate and then heated under the following conditions: temperature: 1300 °C, time: 100 h, gas flow: 30 wt.% water (air:H_2O = 70:30, wt.%), gas flow rate: 175 ml/min. To exclude the water vapor corrosion occurring at low temperatures, the corrosive gas was introduced when the temperature reached 1300 °C and the gas flow was stopped after the 100 h testing period.

Phase identification was made by X-ray diffraction method and surface morphology was observed by Scanning Electron Microscopy (SEM). The phase composition was determined by energy dispersive X-ray (EDX) analysis.

3. Results and discussion

High dense lutetium silicate bulk was successfully prepared by hot-press sintering. The apparent corrosion rate (k_{app}) at 1300 °C was estimated as 1.427×10^{-6} g/cm^2 h.

Fig. 1a and b show the X-ray diffraction patterns of before and after test samples, respectively. Before corrosion, the sample consisted of $Lu_2Si_2O_7$ and Lu_2SiO_5 phases as shown in Fig. 1 (a). It is known that polycrystalline $Ln_2Si_2O_7$ (Ln = rare earth element) possesses large amount of boundary silica. Monteverde and Gelotti reported that 13 mol% excess silica is needed for the preparation of $Ln_2Si_2O_7$ (Ln = rare earth) single phase [7]. In this experiment, the nominal composition of Lu_2O_3 and SiO_2 was exactly stoichiometric composition. Thus, lutetium-rich compound Lu_2SiO_5 phase might be formed according to the amount of the boundary silica mentioned by others. From this argument, and from XRD result, as the sintered sample consisted of $Lu_2Si_2O_7$ and Lu_2SiO_5 crystalline phase and boundary silica, the corrosive behavior of these individual phases should be considered while estimating the corrosion behavior of a bulk sample. Therefore, the apparent corrosion rate must include the corrosion rate for

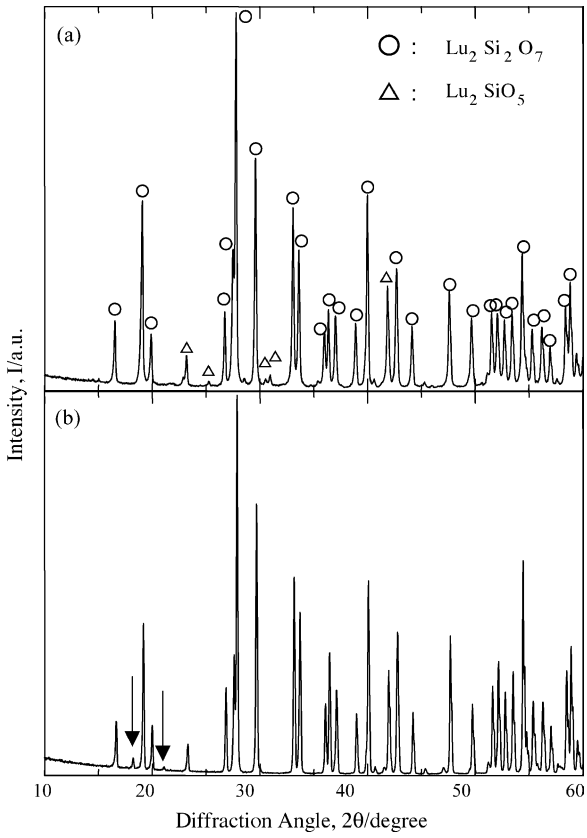

Fig. 1. X-ray diffraction pattern of (a) before and (b) after corrosion test samples.

$Lu_2Si_2O_7$ (k_{227}), Lu_2SiO_5 (k_{215}) and boundary silica (k_S), namely, $k_{app} = k_{227} + k_{215} + k_S$.

In the X-ray diffraction pattern of Fig. 1b, very small peaks were appeared as indicated by arrows. These small peaks were indexed as Lu_2O_3 phase. The phase diagram for Lu_2O_3–SiO_2 binary system has not been established yet, however, it could be considered that the phase diagram of Lu_2O_3–SiO_2 binary system is similar to that of Yb_2O_3–SiO_2 binary system [8]. In the phase diagram of Yb_2O_3–SiO_2 binary system, $Yb_2Si_2O_7$ phase cannot coexist with Yb_2O_3. And the melting points of di-silicate and mono-silicate are higher than 1300 °C, i.e., all stoichiometric compounds in this system are stable under 1300 °C. From this discussion, it can be considered that Lu_2O_3 phase deposited due to the interaction between water vapor and $Lu_2Si_2O_7$ or Lu_2SiO_5 crystalline during the corrosion test.

Fig. 2 shows the typical surface feature found on the surface of after corrosion test. The morphology of the surface was not homogeneous as can be in Fig. 2. Obviously, it can be divided into three types as indicated by dashed line in Fig. 2. The surface features as indicated by I and II were dominant morphology of the sample after corrosion test.

Fig. 3 shows the magnified image of area I. The smooth surface observed in this figure must be attributed to melting down of the surface during corrosion test. In the phase diagram of Yb_2O_3–SiO_2 binary system, the melting points of stoichiometric compounds and all eutectic temperatures are

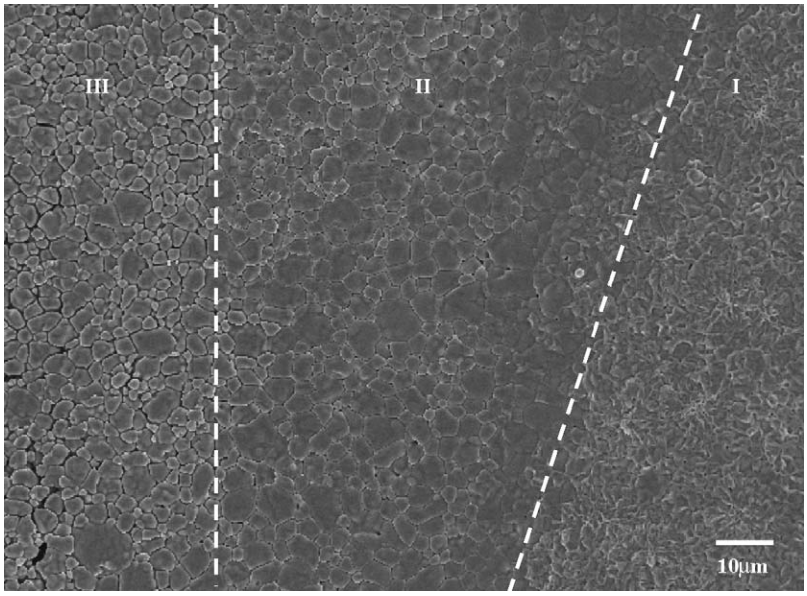

Fig. 2. Typical surface feature found on the after corrosion test sample surface.

higher than 1300 °C. Thus, it can be considered that liquid phase might be formed on the surface by the interaction between water vapor and $Lu_2Si_2O_7$ or Lu_2SiO_5 crystalline.

On the other hand, in area II, individual grains can be clearly seen. Fig. 4 shows magnified image of area II. A peculiar pattern as like as sand ripples or terrace field can be observed on the surface of each grain. This peculiar pattern seems to be the trace of corrosion. Similar kind of peculiar pattern was observed for Al_2TiO_5 phase after water vapor corrosion [9].

In the area III, individual grain can be also clearly seen. However, in this area, the boundary phase was completely removed. And the trace of corrosion as seen in the area II was observed in this area.

The elemental composition of areas I and III was analyzed by EDX method. The estimated compositions of areas I and III were Lu_2O_3:SiO_2 = 1:1.3, and 1:1.93, respectively. No impurity elements were detected in this analysis. It can be recognized that the compositions of areas I and III correspond to that of Lu_2SiO_5 and $Lu_2Si_2O_7$ phases, respectively.

From these above results, it can be considered that Lu_2SiO_5 phase melts down during the corrosion test. As the melting point of Lu_2SiO_5 is higher than 1300 °C, this phase melts due to the interaction with water vapor during corrosion. In the X-ray diffraction pattern as shown in Fig. 1b, a small amount of Lu_2O_3 phase can be identified after the corrosion test. Therefore, three corrosion mechanisms at 1300 °C for

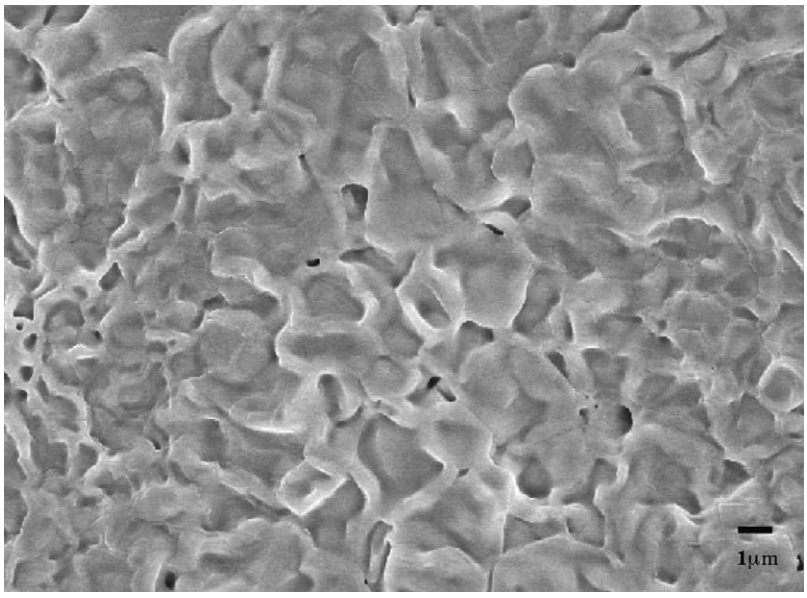

Fig. 3. A high magnification SEM image of area I in Fig. 2.

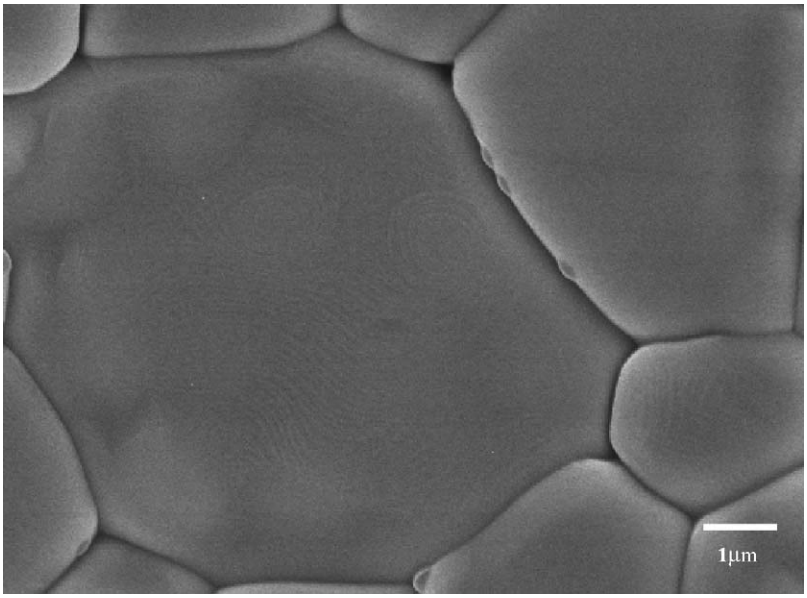

Fig. 4. A high magnification SEM image of area II in Fig. 2.

Lu_2SiO_5 phase can be considered according to Eqs. (1) and (2) and complex of (1) and (2) as follows.

$$Lu_2SiO_5(s) + H_2O(g) \rightarrow Lu_2O_3(s) + SiO_2{\cdot}nH_2O(l) \quad (1)$$

$$2Lu_2SiO_5(s) + H_2O(g) \rightarrow Lu_2Si_2O_7(s) + Lu_2O_3{\cdot}nH_2O(l) \quad (2)$$

As the melting points of SiO_2 and Lu_2O_3 are also higher than 1300 °C, it can be assumed that the melted component include water in the form of $SiO_2{\cdot}nH_2O$ or $Lu_2O_3{\cdot}nH_2O$.

At some places, unique morphology can be observed in area III as shown in Fig. 5. It is seemed that the crystalline phase lying across the grain boundary as indicated by arrow deposited from melted phase. EDX analysis showed all grains in Fig. 5 are $Lu_2Si_2O_7$ phase. Sometimes the melted components could be removed by water vapor as follows.

$$Lu_2O_3{\cdot}nH_2O(l) \rightarrow 2Lu(OH)_3(g)\uparrow \quad (3)$$

$$SiO_2{\cdot}nH_2O(l) \rightarrow Si(OH)_4(g)\uparrow \quad (4)$$

As the composition of area III is $Lu_2Si_2O_7$, it can be considered that the boundary silica is completely removed

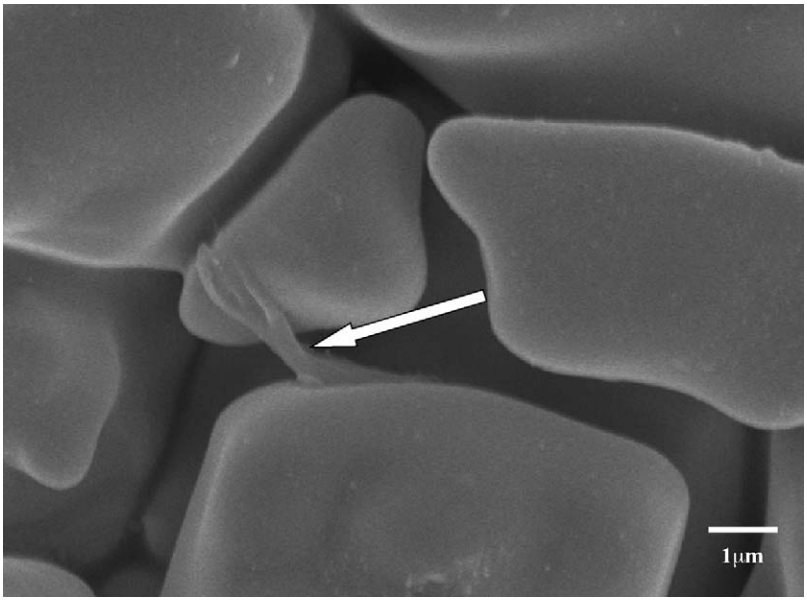

Fig. 5. A unique morphology could be found in area III.

by water vapor from area III. A peculiar pattern as like to sand ripples can be observed on the grain surface only in area II. From these results, the sand ripples pattern as shown in Fig. 4 can be considered as trace of water vapor corrosion. Since the trace of the corrosion was not observed in area III, it is assumed that the water vapor corrosion resistance of $Lu_2Si_2O_7$ crystalline is higher than that of Lu_2SiO_5 phase and boundary silica, namely, $k_{227} \ll k_{215}, k_S$. Thus, it can be considered that the k_{215} and k_S are dominant corrosion mechanisms for polycrystalline $Lu_2Si_2O_7$ phase.

4. Conclusion

$Lu_2Si_2O_7$ phase was well-sustained in the water vapor environment at 1300 °C. Lu_2SiO_5 phase that appeared as a secondary phase in polycrystalline $Lu_2Si_2O_7$ bulk melted down by water vapor attack and easily corroded. The boundary silica phase was also easily removed by water vapor. In the corrosion mechanism of polycrystalline lutetium silicates compound, corrosion of Lu_2SiO_5 and boundary silica phase were dominant.

References

[1] S.M. Wiederhon, M.K. Ferber, Silicon nitride for gas turbines, Curr. Opin. Solid State Mater. Sci. 5 (2001) 311–316.
[2] H.J. Choi, J.G. Lee, Y.W. Kim, High temperature strength and oxidation behavior of hot-pressed silicon nitride-disilicate ceramics, J. Mater. Sci. 32 (1997) 1937–1942.
[3] E.J. Opila, Oxidation and volatilization of silica formers in water vapor, J. Am. Ceram. Soc. 86 (2003) 1238–1248.
[4] E.J. Opila, R.C. Robinson, D.S. Fox, R.A. Wenglarz, M.K. Ferber, Additive effects on Si_3N_4 oxidation/volatilization in water vapor, J. Am. Ceram. Soc. 86 (2003) 1262–1271.
[5] T. Fukudome, S. Tsuruzono, W. Karasawa, Y. Ichikawa, Development and evaluation of ceramic components for gas turbine, Proc. ASME Turbo Expo, 2002, GT-2002-30627.
[6] S. Ueno, D.D. Jayaseelan, N. Kondo, T. Ohji, S. Kanzaki, Preparation and the hydro thermal corrosion resistance of silicon nitride with Lu–Si–O EBC layer at high temperature, J. Ceram. Process. Res. 4 (2003) 214–216.
[7] F. Monteverde, G. Gelotti, Structural data from X-ray powder diffraction of a new phase fromed in the Si_3N_4–La_2O_3–Y_2O_3 system after oxidation in air, J. Eur. Ceram. Soc. 19 (1999) 2021–2026.
[8] J. Felsch, The crystal chemistry of the rare-earth silicates, Struct. Bond. Berl. 13 (1973) 99–197.
[9] S. Ueno, D.D. Jayaseelan, N. Kondo, T. Ohji, S. Kanzaki, High temperature water vapor corrosion behavior of titanium aluminate (Al_2TiO_5), J. Ceram. Soc. Jpn. 111 (2003) 859–861.